Calculation of double-well B vibronic states of SrH

Thierry Leininger and Gwang-Hi Jeung*
Laboratoire de Chimie Quantique, Institut Le Bel, Université Louis Pasteur, 4 rue Blaise Pascal, 67000 Strasbourg, France
(Received 20 September 1993)

The X ($1\,^2\Sigma^+$), A ($1\,^2\Pi$), B ($2\,^2\Sigma^+$), and (1) $^2\Delta$ electronic states of SrH are calculated. A small-core Hartree-Fock pseudopotential for the Sr atom is used together with a large molecular basis set, and extensive valence and core configuration interactions are done. The existence of a double-potential well for the B state, due to an avoided crossing between neutral and ionic configurations, is clearly shown. The dipole moment of this state as a function of the internuclear distance varies greatly, and the vibrational energy levels show an irregular progression. The Einstein coefficients for stimulated absorption for vibronic transitions among these four states are also calculated. This predicts irregular band intensities involving the B state. Spectroscopic data for the (1) $^2\Delta$ state are found, too.

PACS number(s): 31.20.Di, 31.50.+w, 33.10.Gx

I. INTRODUCTION

The electronic states of the alkali hydrides (LiH to CsH) have been the subject of much interest from both experimental spectroscopists and quantum chemists in the past decade (see Ref. [1]). As a result, many excited states, as well as the ground states, of these diatoms are now well known. The excited electronic states of the monohydrides of the alkaline-earth atoms (BeH to BaH) showed complex spectra showing different types of perturbations [2–4]. The low-lying excited states, in particular the A ($1\,^2\Pi$), B ($2\,^2\Sigma^+$), and (1) $^2\Delta$ states are energetically very close. Their mutual interaction is so subtle that to characterize each electronic state required deperturbation processes for the rotational spectra. The absorption intensity for the $v'=v''$ transitions was supposed to be much stronger than other cases, and only the lowest vibrational levels, $v=0,1,2$, have been analyzed to date. These data are insufficient to determine the general shape of the electronic potential curves. The electronic states of the alkaline-earth monohydrides have also been studied by quantum-chemical calculations. These calculations concerned the BeH [5–7], MgH [6–11], CaH [7,12], and BaH [7,13] molecules. One of the most interesting features of these molecules is the presence of a double well in the potential-energy curve of the B state of CaH [12].

The present work reports main spectroscopic properties of the X (ground), A, B, and (1) $^2\Delta$ states of SrH. The presence of a double well for the B state will be shown for the first time. The vibrational analysis is done, using the *ab initio* potential-energy curves. The Einstein coefficients for stimulated absorption for vibronic transitions were calculated from the electronic dipole transition moments and the vibrational wave functions. This resulted in abnormal band progressions and variable intensities involving the B state. We also found the presence of the (1) $^2\Delta$ near the A and B states for the first time.

*Corresponding author.

II. METHOD OF COMPUTATION

The restricted Hartree-Fock (RHF) calculations were done, using the ASTERIX program package [14,15]. The configuration-interaction (CI) calculations was done using a program originally written by Brooks and Schaefer [16], and a direct CI program with contractions by Siegbahn [17]. The graphical unitary-group approach of Paldus [18] and Shavitt [19] was employed in these programs. The small-core relativistic pseudopotential of LaJohn *et al.* [20] was used to simulate the $[1s^2/2s^2 2p^6/3s^2 3p^6 3d^{10}]$ electrons of the Sr atom. The molecular orbitals (MO's) resulting from the RHF calculation of SrH^+ were employed as one-electron basis functions for CI calculations, except for some cases where the canonical MO's were used instead. No MO's were frozen. All configuration-state functions (CSF's) whose weights were greater than 0.001 at each internuclear distance were kept. Then a union of those CSF's was used as a final zeroth-order reference function for each electronic state. The resulting reference CSF's were 3 (Δ state), 4 (X state), 6 (A state), and 15 (B state). All the single- and double substituted CSF's generated from these zeroth-order wave functions were included in the final multireference CI (MRCI). The largest CI included nearly half a million CSF's, which took about 120 min. of CPU time on a CRAY-2 machine to make a distinct row table and to diagonalize in order to calculate the energy of a single state at a given internuclear distance.

First, the $7s7p5d$ Gaussian-type orbitals (GTO's) to best describe the ^1S, ^3P, and ^3D states of the Sr atom were obtained. These were then contracted to $6s6p5d$ atomic basis functions (ABF's) with the contraction coefficients for the ground state. The CI energy of the ^{3}D atomic state changes very slowly as a function of the f GTO exponent, 0.095, giving the lowest energy. The molecular effect of the f GTO was also verified for SrH at $R=4.5$ bohr. The potential energies for the $^2\Delta$ and X states changed little for the variation of the f exponent from 0.05 to 1.0. Consequently, one f GTO with the exponent 0.095 was retained for the molecular calculation. For the hydrogen atom, $5s2p$ GTO's contracted to $3s2p$ ABF's

were used. This basis set gave the electron affinity of the hydrogen atom of 0.65 eV [21], in fairly good agreement with the experimental value 0.75 eV [22]. The $^1S \rightarrow {}^3D$ excitation energy calculated in an extensive CI was 1.79 eV, which agrees well with the experimental value, 1.81 eV [23]. The $^1S \rightarrow {}^3D$ excitation energy was calculated to be 2.50 eV, which is significantly larger than the experimental value, 2.26 eV. The potential energies for the (1) $^2\Delta$ state was translated with respect to the ground state to compensate for this atomic energy difference. The first ionization potential of Sr was calculated to be 5.49 eV, which should be compared with the experimental value, 5.69 eV.

It is not clear at present which one of Hund's cases, *a* or *c*, applies better to the excited states of SrH. The spin-orbit coupling was taken into account through a first-order perturbation method. The molecular wave functions projected into the atomic orbitals and the spin-orbit coupling coefficients extracted from the experimental data were used. The static and transition dipole moments were calculated using the MRCI wave functions. The potential-energy curves, static dipole-moment curves, and transition dipole-moment curves were fitted with cubic spline functions to find equilibrium spectroscopic constants. The products of the vibrational wave functions, $W_{(m,v')}(R)$ and $W_{(n,v'')}(R)$, and the transition dipole moment as a function of the internuclear distance, $\mu_{(n\leftarrow m)}(R)$, were numerically integrated to obtain the vibronic transition dipole moment,

$$p^u_{(nv''\leftarrow mv')} = \int_0^\infty dR\ W^*_{(n,v'')}(R) W_{(m,v')}(R) \mu^u_{(n\leftarrow m)}(R)\ ,$$

where m and n designate the upper and the lower electronic states, respectively, v' and v'' designate the corresponding vibrational states, and u represents the x, y, and z components. Then the Einstein coefficients of stimulated absorption for vibronic transitions [24] were obtained according to

$$B(nv''\leftarrow mv') = \frac{\mu_0 c^2}{6\hbar^2} \sum_u |p^u_{(nv''\leftarrow mv')}|^2\ .$$

Our calculation has its limited accuracy, although we tried to use the best available method at present. Our calculated X-B transition energy is too high by 640 cm^{-1}, in comparison with the experimental estimate, whereas the X-A transition energy is much closer to the experimental value, as will be shown below. However, we believe that the presence of a double well for the B state and the qualitative conclusion regarding the B-X and B-A transition intensities remain valid.

III. RESULT AND DISCUSSION

The potential-energy curves for the X, A, B, and (1) $^2\Delta$ states are drawn in Fig. 1. As the spin-orbit effect is very small, only the $^{2\Sigma+1}\Lambda$ states are presented in this figure.

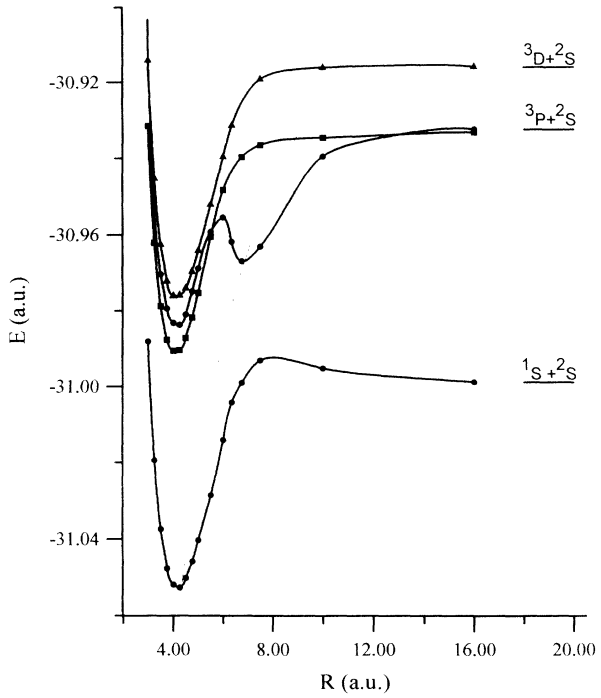

FIG. 1. Potential-energy curves of the lowest electronic states of SrH: X (1) and B (2) $^2\Sigma^+$ states (dots), A (1) $^2\Pi$ state (squares), and (1) $^2\Delta$ state (triangles).

Our molecular calculation at 16 bohr for the ground and excited states gave nearly the same energy as the sum of the CI energies for the Sr atom and the RHF energy for the H atom. Indeed, the differences between the molecular energies and the sum of the atomic energies are 0.09 eV (X), 0.03 eV (A), 0.003 eV (B), and 0.07 eV ($^2\Delta$) at that distance. If we may assume that the molecular states practically correspond to the dissociated atomic states at such distance, it means that our CI calculation does not suffer too much from the size-inconsistency problem.

The X and B states show an avoided crossing at around 7 bohr. This is due to the interaction between the neutral and ionic configurations. This kind of avoided crossing was clearly analyzed for the CaH molecule [12]. An energy barrier is shown to be present for the ground state in Fig. 1. To verify whether this barrier is real, we performed other sorts of calculations. The use of a large-core pseudopotential with extended basis and full valence CI removed the barrier. The use of small-core pseudopotential with minimal basis ($2s2p1d$) and full CI did not show the barrier either. On the other hand, the use of small-core pseudopotential with extended basis and frozen-core ($4s4p$) full valence CI did result in a potential whose height was lower than in Fig. 1. This evidently indicates that the presence of the barrier for the ground state originates from the polarization of $4s$ and $4p$ core electrons, and that the subsequent valence-core and core-core correlations amplify the barrier height. It is not certain whether this barrier is real or whether it is a computational artifact. No such barrier has been found among the alkaline-earth monohydrides and alkali hy-

drides. Similar calculations for CaH [12] and BaH [13] did not reveal such barriers.

The (2) $^2\Sigma^+$ state shows a long-distance potential well (at around 6.8 bohr). The presence of such a second potential well was predicted for CaH at around 6 bohr [12]. The potential-energy curve for the *B* state of the BaH molecule showed a very shallow exterior well at around 7 bohr [13], but it appears uncertain whether this well may contain a bound vibrational state. In contrast, a full valence CI [10] did not show any double well for the MgH molecule. Many avoided crossings arise also between higher-lying electronic states (not reported in this paper) as in the CaH and BaH molecules. But the general shapes of the potential-energy curves of the CaH, SrH, and BaH molecules are quite different.

Our calculated spectroscopic constants are summarized in Table I. The equilibrium characteristics (R_e, ω_e, $\omega_e x_e$, B_0, or B_e) are in fairly good agreement with the existing experimental data [3,25–27]. Our transition energy from the ground state to the *A* state is slightly overestimated in comparison with the experimental data. However, the difference with experimental data is particularly large for the *B*-*X* case. The observed *B*-*A* separation at $v=0$ is about 800 cm^{-1} after deperturbation [4]. Our calculated value for this separation is 1265 cm^{-1}. This disparity may partially originate from a differential core-core correlation. An experimental estimation of the dissociation for the *B* state [25], which was obtained by extrapolation assuming a regular Morse form of the potential curve, is incompatible with the *B*-*X* transition energy and the dissociation energy of the ground state, i.e., $T_e(B-X)+D_e(B)-D_e(X)\neq T_e(^3P\text{-}^1S)$. This may be an indirect experimental proof of the irregular form of the *B* potential curve.

The presence of the (1) $^2\Delta$ state was supposed a long time ago [25]. Our calculation gives spectroscopic data for this state. The proximity of this state to the *A* and *B* states should further complicate the analysis of the spectra for high v values.

The calculated dipole moments as functions of the internuclear distance are shown in Fig. 2. Here, the positive value means a $Sr^{\delta}-H^{\delta+}$ situation and the negative value means a $Sr^{\delta+}H^{\delta-}$ situation. These dipole-moment curves are rapidly varying functions, reflecting a large variation in the nature of the wave functions. All electronic states in Fig. 2 show $Sr^{\delta+}H^{\delta-}$ at long distances ($R>7$ bohr). The *X*, *A*, *B*, and (1) $^2\Delta$ states have linearly changing dipole moments in the internuclear distance range of from 3 to 6 bohr. The *B* state shows a positive dipole moment in the R range of 5.5–6.5 bohr. The inversions of the dipole moment for this state come from a competition of two opposing contributions, the bonding orbital contribution, and the nonbonding or antibonding orbital contribution. At $R=6$ bohr, the total populations of this state at 6 bohr are 1.95 (Sr) and 1.05 (H). The bonding natural orbital shows populations of 0.23 (Sr) and 0.87 (H), and the nonbonding and antibonding natural orbitals show 1.43 (Sr) and 0.16 (H). The contribution to the $Sr^{\delta-}H^{\delta+}$ due to the nonbonding and antibonding orbitals (mainly s-p_σ) is greater than the $Sr^{\delta+}H^{\delta-}$ contribution from the bonding orbital around $R=6$ bohr. The oscillating behavior of the dipole-moment function was previously reported for the *B* state of MgH [10]. Higher-lying states (not reported in this paper) show larger oscillations of the dipole-moment function.

TABLE I. Spectroscopic constants of the low-lying states of SrH.

State	Ω	R_e (pm)	ω_e (cm^{-1})	$\omega_e x_e$ (cm^{-1})	B_0 (cm^{-1})	D_e (eV)	T_e (cm^{-1})	μ_e (a.u.)	Reference
(1) $^2\Delta$	5/2	217	1043	−12	3.46	1.64	16 851	−2.75	This work
	3/2	219	1044	−11	3.46	1.64	16 776		
B (2) $^2\Sigma^+$[a]		220	1288	31	3.47	1.42	14 952	−0.65	This work
		211.7	1234.3	21.1	3.73		14 312.7		Ref. [3]
A (1) $^2\Pi$	3/2	216	1173	13	3.57	1.76	13 804	−1.10	This work
	1/2	216	1175	14	3.52	1.75	13 571		
		212.1	1253.9	18.0	3.72		13 500.6		Ref. [3]
X (1) $^2\Sigma^+$		221	1167	19	3.43	1.47	0	−1.15	This work
		228.8/216.4	1107	26.1		1.56		−1.48	Ref. [7]
		216	1206.2	17	3.63	1.49			Ref. [25]
		214.6	1207.0	17.1	3.67[b]				Ref. [3]
		214.6	1206.9	17.0	3.67[b]				Ref. [26]
		214.6	1205.6	17.1	3.67[b]				Ref. [27]

[a]Reference [25] gives $B_0=3.83$ cm^{-1} and $D_e=1.52$ eV.
[b]B_e values.

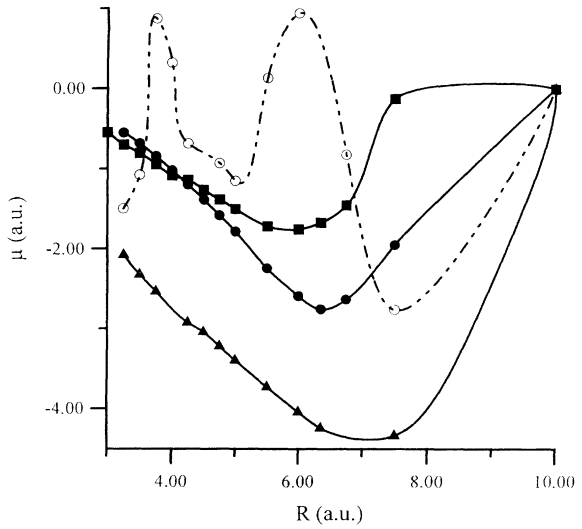

FIG. 2. Dipole-moment curves, μ_{mm}, for the lowest electronic state of SrH: X (dots), A (squares), B (circles), and (1) $^2\Delta$ state (triangles). Positive values signify $Sr^{-\delta}H^{+\delta}$ and negative values signify $Sr^{+\delta}H^{-\delta}$.

The vibrational levels of the B state show an irregular progression due to the presence of the second potential well as can be seen in Fig. 3. The vibrational states for $v=0,1,2$ are exclusively localized in the interior well. The $v=3$ and 4, $v=5$ and 6, and $v=7$ and 8 pair states are practically degenerate. The $v=3$ and 5 states are largely localized in the interior well, while the $v=4$ and 6 states are largely localized in the exterior well. The $v=7$ state is principally localized in the interior well. However, it has non-negligible probability of finding itself in the exterior well. The reverse is true for the $v=8$ state. The vibrational wave functions for $v=7$ and 8 are shown in Fig. 3. All states with $v>8$ are delocalized as they lie above the potential maximum.

The transition dipole moments as functions of the internuclear distance, $\mu^{\mu}_{(n\leftarrow m)}$, for the $A\leftarrow X$, $B\leftarrow X$, $B\leftarrow A$, and (2) $^2\Delta\leftarrow A$ transitions are drawn in Fig. 4. The transition dipole moment for $B\leftarrow X$ as a function of the internuclear distance shows small-amplitude oscillations in the range of 4–6 bohr. These oscillations probably originate from the incomplete convergence of MRCI electronic wave functions. In fact, it is more difficult to get well-converged wave functions than it is to get well-converged energies.

The Einstein coefficients of stimulated absorption for vibronic transitions, $V_{(nv'\leftarrow mv'')}$, are drawn in Fig. 5. All possible transitions between $0\le v'\le 9$ and $0\le v''\le 9$ appear in this figure. The Einstein coefficients for $A\leftarrow X$ [Fig. 5(a)] and (1) $^2\Delta\leftarrow A$ [Fig. 5(b)] are much larger than those of $B\leftarrow X$ [Fig. 5(d)] and $B\leftarrow A$ [Fig. 5(c)]. As the density of rotational and vibrational states are of the same order of magnitude for the A and B states, the absorption intensities for $A\leftarrow X$ should be much stronger than those of $B\leftarrow X$. The Einstein coefficients for $A\leftarrow X$ and (1) $^2\Delta\leftarrow A$ are typical: the $\Delta v\equiv|v'-v''|=0$ transitions (diagonal) have large probabilities of transition whereas the off-diagonal terms have vanishingly small values. The same pattern is found in the overlap of vibrational functions only, i.e., the Franck-Condon factors (FCF's). In contrast, the Einstein coefficients for $B\leftarrow X$ and $B\leftarrow A$ show many strong extradiagonal transitions. The distribution of the transition probability does not match that of the FCF's [Fig. 5(f)] this time. Unfortunately, the experimental information on these electronic systems remains incomplete and cannot confirm this unusual distribution.

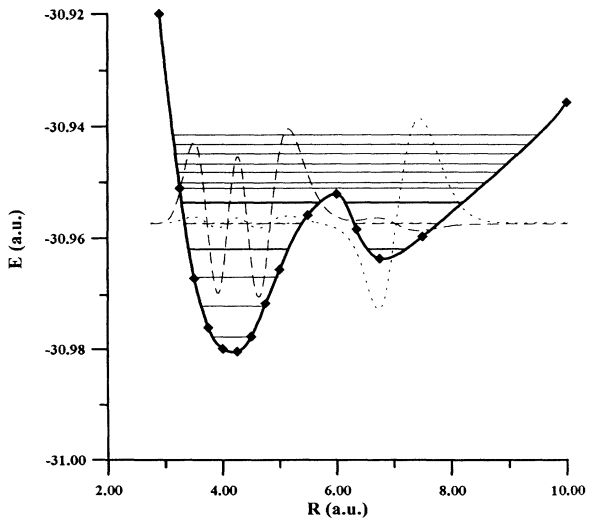

FIG. 3. Vibrational energy levels for $v=0$-14 and vibrational wave functions (in arbitrary amplitudes) for $v=5$ (dashed curve) and $v=6$ (dotted curve) of the B state.

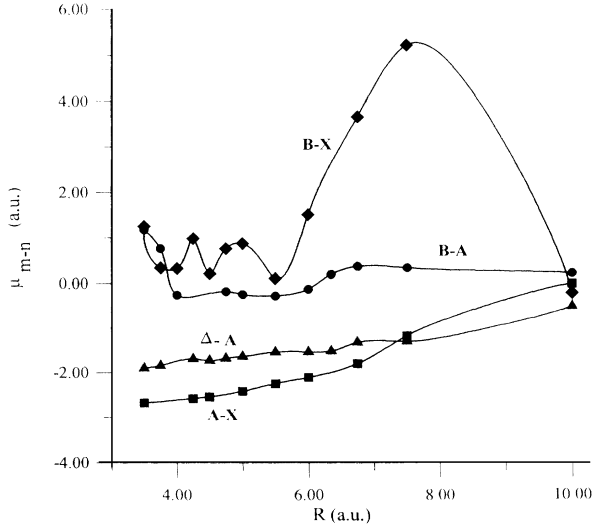

FIG. 4. Transition dipole-moment amplitude curves, $\mu^{\mu}_{(n\leftarrow m)}$, for the A-X (squares), B-A (diamonds), B-A (dots), and (1) $^2\Delta$-A (triangles).

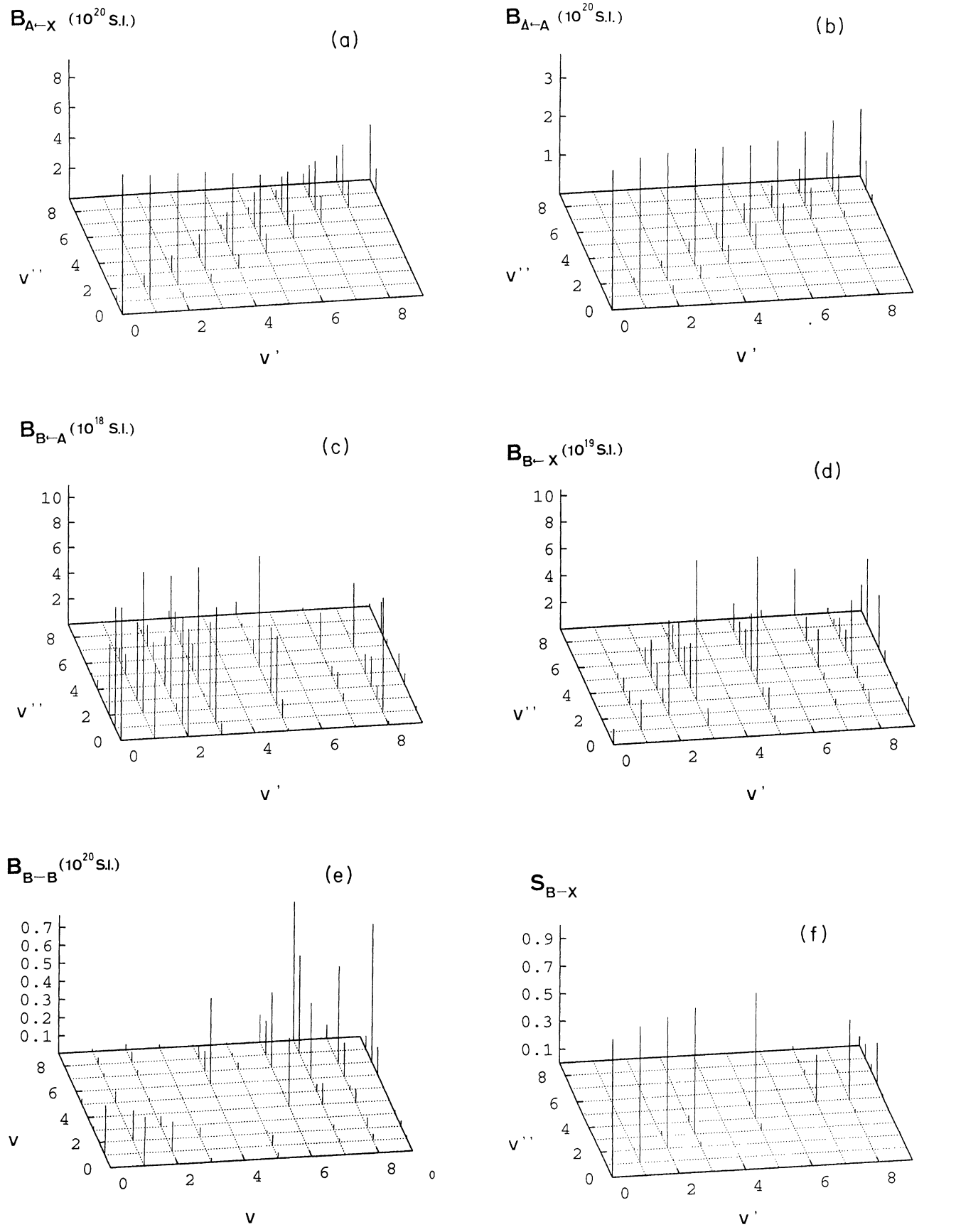

FIG. 5. Einstein coefficients for stimulated absorption, $B_{(n\leftarrow m)}$, for vibronic transitions $A\leftarrow X$ (a), $(1)\,^2\Delta\leftarrow A$ (b), $B\leftarrow A$, (c), $B\leftarrow X$ (d), and B-B (e), in $J^{-1}m^3s^{-2}$, (S.I. units), and B-X Franck-Condon factors (f).

ACKNOWLEDGMENTS

The calculation presented in this work was done with the CRAY-2 machine of the CCVR at Palaiseau and the IBM-3090 machine of the CCSC near Strasbourg through a grant from the CNRS. Many valuable discussions with Dr. A. J. Ross, Dr. R. F. Barrow, and Professor W. C. Stwalley are gratefully acknowledged. The Laboratoire de Chimie Quantique is "Unité Propre No. 139 au Centre National de la Recherche Scientifique."

[1] W. C. Stwalley, W. T. Zemke, and S. C. Yang, J. Phys. Chem. Ref. Data **20**, 153 (1991).

[2] H. Martin, J. Chem. Phys. **88**, 1797 (1988).

[3] O. Appelblad, L. Klynning, and J. W. C. Johns, Phys. Scr. **33**, 415 (1986).

[4] A. Bernard, C. Effantin, J. d'Incan, G. Fabre, R. Stringat, and R. F. Barrow, Molec. Phys. **67**, 1 (1989).

[5] P. Politzer, J. D. Elliott, and B. F. Meroney, Chem. Phys. Lett. **23**, 331 (1973).

[6] W. Meyer and P. Rosmus, J. Chem. Phys. **63**, 2356 (1975); P. Rosmus and W. Meyer, *ibid.* **66**, 13 (1977).

[7] P. Fuentealba, O. Reyes, H. Stoll, and H. Preuss, J. Chem. Phys. **87**, 5338 (1987); P. Fuentealba, A. Savin, H. Stoll, and H. Preuss, Phys. Rev. A **40**, 2163 (1989); **41**, 1238 (1990); M. Kaupp, P.v.R. Schleyer, H. Stoll, and H. Preuss, J. Chem. Phys. **94**, 1360 (1991).

[8] P. E. Cade and W. M. Huo, J. Chem. Phys. **47**, 649 (1967); P. E. Cade, R. F. W. Bader, W. H. Hennecker, and I. Keaveny, J. Chem. Phys. **50**, 5313 (1969).

[9] A. C. H. Chan and E. R. Davidson, J. Chem. Phys. **52**, 4108 (1970).

[10] R. P. Saxon, K. Kirby, and B. Liu, J. Chem. Phys. **69**, 5301 (1978).

[11] W. H. Henneker and H. Popkie, J. Chem. Phys. **54**, 1763 (1971).

[12] G. H. Jeung, J. P. Daudey, and J. P. Malrieu, Chem. Phys. Lett. **98**, 433 (1983).

[13] A. R. Allouche, G. Nicolas, J. C. Barthelat, and F. Spiegelmann, J. Chem. Phys. **96**, 7646 (1992).

[14] R. Ernenwein, M. M. Rohmer, and M. Bénard, Comput. Phys. Commun. **58**, 305 (1990); M. M. Rohmer, J. Demuynck, M. Bénard, R. Wiest, C. Bachmann, C. Henriet, and R. Ernenwein, *ibid.* **60**, 127 (1990); M. M. Rohmer, R. Ernenwein, M. Ulmschneider, R. Wiest, and M. Bénard, Int. J. Quantum Chem. **40**, 723 (1991).

[15] T. Leininger, G. H. Jeung, M. M. Rohmer, and M. Pélissier, Chem. Phys. Lett. **190**, 342 (1992).

[16] B. R. Brooks and H. F. Schaefer, III, J. Chem. Phys. **70**, 5092 (1979).

[17] P. E. M. Siegbahn, J. Chem. Phys. **72**, 1647 (1980).

[18] J. Paldus, J. Chem. Phys. **61**, 5321 (1974).

[19] I. Shavitt, Int. J. Quantum Chem. Symp. **11**, 131 (1977).

[20] L. A. LaJohn, P. A. Christiansen, R. B. Ross, T. Atashroo, and W. C. Ermler, J. Chem. Phys. **87**, 2812 (1987).

[21] G. H. Jeung, J. P. Daudey, and J. P. Malrieu, J. Phys. B **16**, 699 (1983).

[22] A. A. Radzig and B. M. Smirnov, *Reference Data on Atoms, Molecules, and Ions* (Springer, Berlin, 1985), p. 131.

[23] C. E. Moore, *Atomic Energy Levels,* Natl. Bur. Stand. (U.S.) Circ. No. 467 (U.S. GPO, Washington, D.C., 1971), Vols. 1–3.

[24] E. Durand, *Mécanique Quantique* (Masson, Paris, 1970), Vol. 1, pp. 572–576.

[25] W. W. Watson and W. R. Fredrickson, Phys. Rev. **39**, 765 (1932); W. W. Watson, W. R. Fredrickson, and M. E. Hogan, *ibid.* **49**, 150 (1936); R. F. Humphreys and W. R. Fredrickson, *ibid.* **50**, 542 (1936).

[26] U. Magg, H. Birk, and H. Jones, Chem. Phys. Lett. **151**, 263 (1988).

[27] H. Birk, R.-D. Urban, P. Polomsky, and H. Jones, J. Chem. Phys. **94**, 5435 (1991).